GLOBAL JOURNAL OF ENGINEERING RESEARCH VOL. 4 NO. 1&2, 2005: 49 - 61
COPYRIGHT(C) BACHUDO SCIENCE CO. LTD. PRINTED IN NIGERIA. ISSN 1596-292X

A RECEDING EVAPORATIVE FRONT MODEL FOR THE DRYING CHARACTERISTICS OF A FLAT PLATE III: PRESSURE AND MOISTURE DISTRIBUTIONS

Y. T. PUYATE

(Received 30 January 2004; Revision accepted 20 July 2005)

ABSTRACT

A composite model is presented for the pressure and moisture distributions during a three-stage drying process of a flat plate with a fixed base. In the first stage (saturated stage), the body is fully saturated and capillary flow prevails. During the second stage (partially saturated stage), the evaporative front recedes through the material and divides it into saturated and unsaturated regions. The saturated part of the body is modelled using Darcy's Law for pressure-driven flow, while the unsaturated part is characterized by a Fickian diffusion equation, where the pressure model and the diffusion model are coupled through the receding evaporative front. In the third stage (fully unsaturated stage), the saturated region of the partially saturated stage is obliterated and the body is entirely unsaturated. It is shown that the critical point can occur in either the partially saturated stage or the fully unsaturated stage, depending upon the evaporation rate and other parameters of the drying process; both the pressure in the liquid and the moisture concentration of the body increase with distance from the drying face at any given time.

KEYWORDS: Drying, Pressure, Moisture, Distribution, Flat plate.

INTRODUCTION

The theory on the drying characteristics of a flat plate, which includes a proposed three-stage drying process for porous materials, is presented in Part I of this series (Puyate, 2003a). Models for the stress and strain produced during drying of a flat plate with a fixed base in which the receding evaporative front is accounted for, are presented in Part II (Puyate, 2003b). In the first stage (saturated stage) of the proposed three-stage drying process, the body is fully saturated and pressure-driven flow prevails. During the second stage (partially saturated stage), the evaporative front recedes into the material and divides it into two regions; the interior of the material remains saturated up to the evaporative front, while the exterior part of the material is unsaturated. During the third stage (fully unsaturated stage), the saturated region of the partially saturated stage is obliterated and the body becomes fully unsaturated; moisture transport within the body during this stage is by diffusion only.

Scherer (1987b) has developed a capillary flow model for the pressure distribution during drying of a flat plate. Darcy's Law was applied to derive a diffusion equation for the pressure in the liquid, which was solved using a two-stage model. In the first part of the model (the constant-rate period), the evaporation rate is constant and the capillary tension within the liquid rises. A critical point is reached when the capillary tension reaches a maximum value at the free surface, and this marks the end of the first stage. In the second stage of the model (the falling-rate period), the capillary tension at the free surface remains fixed at the maximum value and the drying rate gradually decreases. In this approach, the drying front is effectively pinned at the free surface as the falling-rate period progresses, which is inconsistent with reality and literature (e.g. Puyate, 2003a). Although the liquid may be partly funicular in the early stages of the falling-rate period, not all the pores are completely full of liquid so the permeability of the material will depend on the moisture content (Scheiddegger, 1974). The use of the pressure model developed by Scherer (1987a, 1987b, 1990) with constant permeability for the falling-rate period raises concern, especially when pockets of liquid become isolated and the liquid can be transported from the interior of the body to the surface only by diffusion of its vapour.

Earlier models for drying following from the work of Sherwood (Sherwood, 1931; Gilliland and Sherwood, 1933), were based on mass transfer of moisture by diffusion within the porous medium. In these models, no account is taken of the capillary tension or the receding evaporative front. There is a constant-rate period in which the evaporation rate is constant and the moisture content of the body falls. The moisture content at the free surface falls to its equilibrium value at the end of the constant-rate period, and remains constant during the subsequent falling-rate period until the material is completely dry. Sherwood's model for the constant-rate period (Gilliland and Sherwood, 1933) has also been shown by Puyate (1999, 2003a) to give reasonable results with experimental data. However, Sherwood's models for the falling-rate period (Sherwood, 1931) do not describe adequately the drying kinetics of a body for all values of a parameter called "drying intensity" (Puyate, 1999, 2003a). An improved model for the falling-rate period based on Sherwood's diffusion theory, which is valid for all values of the drying intensity, is presented in Puyate (2003a).

Y. T. PUYATE, Dept. of Chemical Engineering, Rivers State University of Science and Technology, Port Harcourt, Port Harcourt, Nigeria

Editor's Note: This paper was earlier printed in Vol. 3 (1&2) P. 83-91, 2004. it is being reprinted here because of omission of Figs. 1-5

Scherer's (1987a, 1987b, 1990) and Sherwood's (Sherwood, 1931; Gilliland and Sherwood, 1933) models for drying are both quite widely used, yet are based on quite different paradigms. The Scherer model is based on capillary flow and is clearly appropriate for the initial stage of drying when the body is saturated, and is also valid within the saturated region of the partially saturated stage. The Sherwood model is based on moisture diffusion through the porous body and is clearly appropriate when the body is nearly dry, the pores are filled mostly with air, and the liquid exists in isolated pendular drops. Neither model is entirely satisfactory, though both have been used to describe the entire drying process of a body from the initial stage to dryness.

This paper presents a composite model for pressure flow and moisture diffusion during a three-stage drying process of a flat plate with a fixed base, where the pressure model and the diffusion model are coupled through the receding evaporative front. The diffusion model is used to describe the flux of moisture in the unsaturated region, while the pressure model is used for the flux in the saturated region.

The model

In the present paper (and unlike Scherer's analysis), when the capillary tension reaches its maximum value at the exterior surface of a body, the evaporative front is drawn into the material and the body is only partially saturated. The evaporation rate remains constant for a further period, until the moisture concentration at the surface approaches the equilibrium moisture concentration. The equations for saturated flow prevail in the saturated region of the body, and the capillary tension at the evaporative front remains at the maximum value as the evaporative front recedes into the material. Mass transfer in the unsaturated region is by diffusion and follows a Fickian equation originally developed by Sherwood (1929). Eventually, the moisture concentration at the surface of the body falls to the equilibrium value. This marks the critical point of the drying process and the end of the constant-rate period. (Traditionally (Gilliland and Sherwood (1933)), the constant-rate period is taken to end when the moisture concentration at the surface of a body falls to the equilibrium value). Thereafter, the surface moisture concentration remains at the equilibrium value and the falling-rate period begins. The critical point can occur in either the partially saturated stage or the fully unsaturated stage, depending on the evaporation rate and other parameters of the drying process.

Pressure and moisture distributions

In this section, models for the pressure and moisture distributions in the three stages of drying are presented for the one-dimensional drying of a flat plate with a fixed base. The receding evaporative front is accounted for in the models; Darcy's Law is used to describe saturated pressure-driven flow, while mass transport in the unsaturated region is characterized by a Fickian diffusion equation.

Stage 1: Saturated stage

During the saturated stage, the pores are full of liquid so Darcy's Law holds, and the governing equation for the pressure distribution is given by (Puyate, 2003b)

$$\frac{\partial P_L}{\partial t} = D\frac{\partial^2 P_L}{\partial z^2} \qquad 0 < z < L \qquad (1)$$

where z is the distance measured in the direction of fluid flow, L is the thickness of the plate, t is time, P_L is the gauge pressure (Puyate, 2003a,b) in the liquid, and D is a transport coefficient defined in Puyate (2003b). Initially, the free surface of the plate is covered with a film of liquid (flat surface) so the capillary tension in the liquid is zero, and $P_L = 0$. Since the rate of evaporation is constant during the saturated stage, the evaporative flux must balance the pressure flux at the free surface ($z = L$), while the pressure flux at the unexposed face ($z = 0$) is zero. The initial and boundary conditions of eq. (1) for the saturated stage may then be expressed as

$$t = 0: \qquad P_L = 0 \qquad (2a)$$

$$z = 0: \qquad \frac{\partial P_L}{\partial z} = 0 \qquad (2b)$$

$$z = L: \qquad \frac{\partial P_L}{\partial z} = -\frac{\alpha \eta_L}{\rho_L \kappa} \qquad (2c)$$

where α is the rate of evaporation per unit area in the constant-rate period, κ is the permeability of the plate, and ρ_L is the density of the liquid. The saturated stage ends when P_L falls to a minimum value $P_{\min}$ at the surface, corresponding to a maximum capillary tension $\varphi_{\max}$ (Puyate, 2003b). Thereafter, the menisci recede into the pores and the partially saturated stage begins.

Stage 2.: Partially saturated stage

In this stage of drying, the plate is divided by the receding evaporative front into two zones; the exterior of the plate from the surface to the evaporative front is unsaturated, while the interior of plate from the evaporative front to the unexposed face is saturated. Equation (1) applies to the saturated zone, while mass transport in the unsaturated region is modelled by a Fickian diffusion equation. The initial condition of the saturated region of the partially saturated stage corresponds to the pressure distribution at the end of the saturated stage, with P_L equal to P_{min} at the drying surface; the pressure at the interior evaporative front remains at P_{min} as the evaporative front retreats into the body.

With the assumption that the rate of evaporation remains constant until the moisture concentration at the surface of the plate falls to the equilibrium value, the equations describing the two zones of the partially saturated stage may then be expressed as

Unsaturated zone

$$\frac{\partial \rho}{\partial t} = D_m \frac{\partial^2 \rho}{\partial z^2} \qquad z_i(t) < z < L \qquad (3)$$

with the conditions

$$t = t_E: \qquad \rho = \chi \phi \rho_L \qquad (4a)$$

$$z = z_i(t): \qquad \rho = \chi \phi \rho_L \qquad (4b)$$

$$z = L: \quad \begin{cases} \text{CRP}: & \dfrac{\partial \rho}{\partial z} = -\dfrac{\alpha}{D_m} \\ \text{or} & \\ \text{FRP}: & \rho = \rho_{eq} \end{cases} \qquad (4c)$$

Saturated zone

$$\frac{\partial P_L}{\partial t} = D \frac{\partial^2 P_L}{\partial z^2} \qquad 0 < z < z_i(t) \qquad (5)$$

with the conditions

$$t = t_E: \qquad P_L = P_E(z, t_E) \qquad (6a)$$

$$z = 0: \qquad \frac{\partial P_L}{\partial z} = 0 \qquad (6b)$$

$$z = z_i(t): \qquad P_L = P_{min} \qquad (6c)$$

where CRP and FRP mean constant-rate period and falling-rate period respectively, t_E is the time for the end of the saturated stage (the entry time), $P_E(z, t_E)$ is the pressure distribution at the end of the saturated stage, $z_i(t)$ is the time-dependent interface (evaporative front) position assumed to be sharp, ρ is the mass concentration of moisture, D_m is the moisture diffusion coefficient that is derived from data in the falling-rate period (Puyate, 1999), ϕ is the porosity of the plate, and ρ_{eq} is the equilibrium moisture concentration. The shrinkage of the plate is assumed to be small, so that the porosity is taken to be constant. Note that at the inception of the partially saturated stage, the extent of the unsaturated zone is infinitesimal, so that the initial condition (4a) must be the same as the boundary condition (4b); the factor χ (less than unity) represents the degree to which the pores are filled with liquid in the unsaturated

region immediately adjacent to the saturated region. The saturated and unsaturated regions of the partially saturated stage may be coupled through a continuity of flux condition at the evaporative front, with which, the motion of the evaporative front can be determined. However, a more useful expression may be obtained from the boundary condition (6c), which may be differentiated with respect to time to give the rate of change of the position of the evaporative front as

$$\dot{z}_i(t) = -\frac{D}{L}\left(\frac{\partial^2 P_L / \partial z^2}{\partial P_L / \partial z}\right)_{z=z_i(t)} \tag{7}$$

where the superscript dot indicates the derivative with respect to time. The initial condition for the location of the evaporative front is

$$t = t_E: \qquad z_i(t_E) = L \tag{8}$$

The partially saturated stage ends when the evaporative front reaches the unexposed face of the plate, where $z_i(t) = 0$, and the saturated region is obliterated.

Stage 3: Fully unsaturated stage

This is the stage when no part of the plate is saturated. During this stage, the liquid exists in the pendular state and evaporation occurs within the plate, with vapour diffusing from the interior of the plate to the surface. Depending upon the parameters of the process and the time taken for the moisture concentration at the surface to reach the equilibrium value, the rate of evaporation could remain constant into the fully unsaturated stage. The initial condition for this stage corresponds to the moisture distribution at the end of the partially saturated stage. The defining equation and conditions of the fully unsaturated stage may then be expressed as

$$\frac{\partial \rho}{\partial t} = D_m \frac{\partial^2 \rho}{\partial z^2} \qquad 0 < z < L \tag{9}$$

with the conditions

$$t = t_U: \qquad \rho = \rho_U(z, t_U) \tag{10a}$$

$$z = 0: \qquad \frac{\partial \rho}{\partial z} = 0 \tag{10b}$$

$$z = L: \quad \begin{cases} \text{CRP}: & \dfrac{\partial \rho}{\partial z} = -\dfrac{\alpha}{D_m} \\ \text{or} & \\ \text{FRP}: & \rho = \rho_{eq} \end{cases} \tag{10c}$$

where t_U is the time for the end of the partially saturated stage, and ρ_U is the moisture distribution at the end of the partially unsaturated stage.

3. Solution for drying of a flat plate with a fixed base

The system of equations and the accompanying conditions described in section 2.1 are made dimensionless using the following change of variables

$$\theta = \frac{\rho - \rho_{eq}}{\chi\phi\rho_L - \rho_{eq}} \qquad F = \frac{P_L}{P_{min}} \qquad Z = \frac{z}{L}$$

$$Z_i(\tau) = \frac{z_i(t)}{L} \qquad \tau = \frac{tD_m}{L^2} \tag{11}$$

The dimensionless time τ is expressed in terms of D_m rather than D, since the entire drying process can be modelled in terms of D_m only (Sherwood, 1931; Gilliland and Sherwood, 1933; Puyate, 1999). Note that since both P_L and P_{min} are negative, F is positive. Using eq. (11) in eqs. (1) to (10) gives a set of dimensionless equations in

each of the three stages of drying. In order to fix the size of the saturated and unsaturated regions of the partially saturated stage, Z is rescaled by $Z_i(\tau)$ in the saturated region, and by $1-Z_i(\tau)$ in the unsaturated region in the form

$$\zeta = \frac{Z}{Z_i(\tau)} \qquad \xi = \frac{1-Z}{1-Z_i(\tau)} \qquad (12)$$

where ζ and ξ are new dimensionless spatial variables. The problem is a complex one, with three independent parameters (β, λ, and μ), whose values for experimental conditions are difficult to determine. Furthermore, the model is new and no other work exists for comparison. For these reasons, a detailed study is not attempted here, but will be left as focus of further work. Instead, the solution is considered for two particular cases: (1) when the critical point occurs in the second (partially saturated stage), and (2) when the critical point occurs in the third (fully unsaturated stage).

Case 1. When the critical point occurs in the partially saturated stage

Stage 1. Saturated stage

The location of the critical point does not affect the pressure distribution in the saturated stage since the moisture concentration at the surface of the body exceeds the equilibrium value during this stage of drying. Using ζ from eq. (12) in the dimensionless form of eq. (1) gives the rescaled dimensionless transport equation in this stage as

$$\frac{\partial F}{\partial \tau} = \beta \frac{\partial^2 F}{\partial \zeta^2} \qquad 0 < \zeta < 1 \qquad (13)$$

with the corresponding conditions

$$\tau = 0: \qquad F = 0 \qquad (14a)$$

$$\zeta = 0: \qquad \frac{\partial F}{\partial \zeta} = 0 \qquad (14b)$$

$$\zeta = 1: \qquad \frac{\partial F}{\partial \zeta} = \lambda \qquad (14c)$$

where $\beta = D/D_m$ is the ratio of the transport coefficients in the saturated and unsaturated regions of the plate. One would expect that capillary flow is a more effective transport mechanism than vapour diffusion, so that β may be typically greater than unity. The quantity $\lambda = \alpha\eta_L L/|P_{cap}|\rho_L K$ is a dimensionless evaporation rate (or drying intensity) that relates the characteristic times for evaporation and liquid flow. When λ is large, evaporation is fast, large pressure gradients occur, and the saturated stage is short. Conversely, when λ is small, evaporation is slow, the pressure gradients are small, and the saturated stage is long. During the saturated stage, the evaporative front remains at the surface of the plate so that $Z_i(\tau) = 1$ and $\zeta = Z$. The saturated stage ends at $\tau = \tau_E$, when F increases to unity at $Z = 1$.

In order to match the pressure distribution of the saturated stage at τ_E with the initial condition of the saturated zone of the partially saturated stage, eq. (13) has been solved numerically using conditions (14). Figure 1 shows a plot of F against Z for increasing values of τ, representing the pressure distribution in the plate during the saturated stage. In this and subsequent figures, the parameter values used are $\beta = 2$ and $\lambda = 1$, for which $\tau_E = 0.333$ (determined numerically). The dimensionless variable F represents the tension in the liquid, so the pressure in the liquid will be high in the region of low tension, and vice versa. Thus, the pressure distribution represented in Fig. 1 is non-uniform, with higher pressure further from the drying surface.

Stage 2: Partially saturated stage

The rescaled dimensionless transport equations in the unsaturated and saturated zones of this stage are obtained by using ξ and ζ from eq. (12) in the dimensionless form of eqs. (3) and (5), and in the dimensionless form of conditions (4) and (6), as follows.

Unsaturated zone

$$\frac{\partial\theta}{\partial\tau}+\left(\frac{\dot{Z}_i(\tau)}{1-Z_i(\tau)}\xi\right)\frac{\partial\theta}{\partial\xi}=\frac{1}{(1-Z_i(\tau))^2}\frac{\partial^2\theta}{\partial\xi^2} \qquad 0<\xi<1 \qquad (15)$$

with the conditions

$$\tau=\tau_E: \qquad \theta=1 \qquad (16a)$$

$$\xi=0: \quad \begin{cases} \text{CRP}: & \dfrac{\partial\theta}{\partial\xi}=\mu(1-Z_i(\tau)) \\ \text{or} & \\ \text{FRP}: & \theta=0 \end{cases} \qquad (16b)$$

$$\xi=1: \qquad \theta=1 \qquad (16c)$$

where $\mu=\alpha L/(\chi\phi\rho_L-\rho_{eq})D_m$ is a drying intensity which relates the characteristic times for evaporation and liquid diffusion. When μ is large, evaporation is fast, large concentration gradients occur, and the constant-rate period is short. Conversely, when μ is small, evaporation is slow, the concentration gradients are small, and the constant-rate period is long.

Saturated zone

$$\frac{\partial F}{\partial\tau}-\left(\frac{\dot{Z}_i(\tau)}{Z_i(\tau)}\zeta\right)\frac{\partial F}{\partial\zeta}=\frac{1}{Z_i^2(\tau)}\frac{\partial^2 F}{\partial\zeta^2} \qquad 0<\zeta<1 \qquad (17)$$

with the corresponding conditions

$$\tau=\tau_E: \qquad F=F_E(\zeta,\tau_E) \qquad (18a)$$

$$\zeta=0: \qquad \frac{\partial F}{\partial\zeta}=0 \qquad (18b)$$

$$\zeta=1: \qquad F=1 \qquad (18c)$$

The rescaled form of eq. (7) which is used to update the position of the evaporative front becomes

$$\dot{Z}_i(\tau)=-\frac{\beta}{Z_i(\tau)}\left(\frac{\partial^2 F/\partial\zeta^2}{\partial F/\partial\zeta}\right)_{\zeta=1} \qquad (19)$$

with the initial condition

$$\tau=\tau_E: \qquad Z_i(\tau_E)=1 \qquad (20)$$

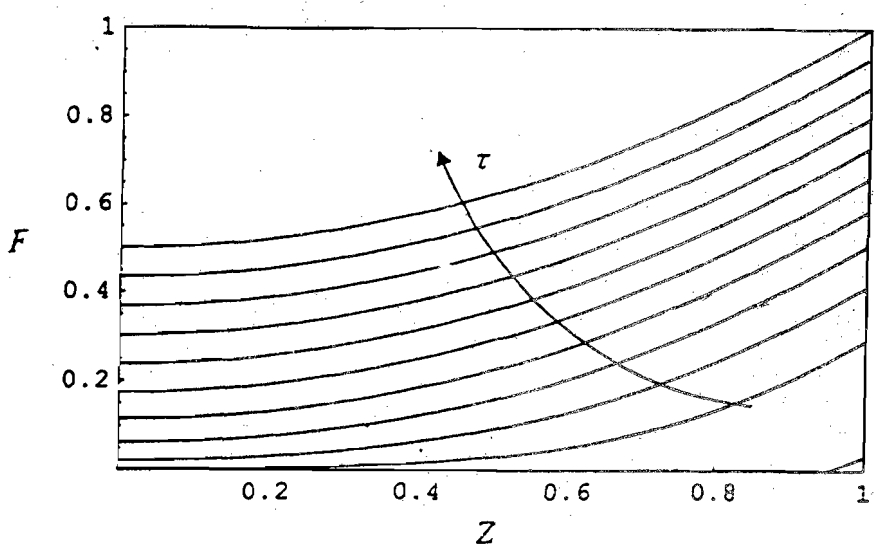

Fig. 1. Pressure distribution during the saturated stage.

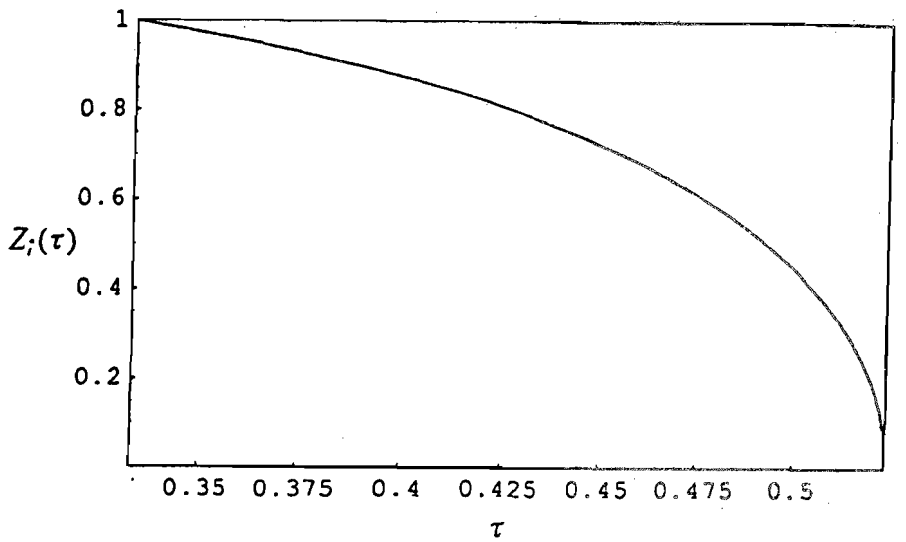

Fig. 2. Evolution of the evaporative front position in the partially saturated stage

It may be seen from eq. (19) that the velocity of the evaporative front depends on β and the form of F. Figure 2 shows the transient evolution of the evaporative front from the end of the saturated stage to the end of the partially saturated stage. It may be seen from Fig. 2 that the partially saturated stage ends when $\tau_U \approx 0.523$.

As the evaporative front recedes into the plate after the dimensionless entry time τ_E, the interior of the plate between the unexposed face and the evaporative front remains saturated until the evaporative front reaches $Z = 0$ at $\tau = \tau_U$. The pressure distribution at the start of the partially saturated stage corresponds to that at the end of the saturated stage, and the pressure at the drying front remains at P_{min} ($F = 1$) as it recedes through the plate. Equation (17) with conditions (18) can then be solved numerically to obtain the pressure distribution in the saturated zone of the partially saturated stage for the period from τ_E to τ_U as shown in Fig. 3.

Stage 2(a): Constant-rate period

The location of the critical point depends upon the drying intensity μ (in relation to β and λ), since τ is expressed in terms of D_m. When μ is large, the constant-rate period is short and the critical point occurs in the partially saturated stage; this case is illustrated here using the parameter values of $\beta = 2$, $\lambda = 1$, and $\mu = 3.5$. The constant-rate period continues from the saturated stage into the partially saturated stage, so eq. (15) can be solved numerically using conditions (16a), (16b) (for CRP), and (16c). The constant-rate period ends when the moisture concentration at the surface of the plate falls to the equilibrium value; that is $\theta = 0$ at $Z = 1$. Figure 4 shows a plot of θ_0 (the moisture

concentration at the surface of the plate) against τ in the dimensionless time range $\tau_E \le \tau \le \tau_U$. It may be seen from Fig. 4 that θ_0 drops to zero at $\tau_{CR} \approx 0.493$ (obtained numerically), where τ_{CR} is the dimensionless critical time. Figure 5 shows a plot of θ against Z for a range of values of τ from τ_E to τ_{CR}. Thus the moisture distribution during the constant-rate period is uneven, with higher moisture further from the drying face. The moisture concentration at the interior of the evaporative front remains at $\theta = 1$ (the fractional saturation of the pores) and the pressure remains at $F = 1$ as the evaporative front recedes through the material during the partially saturated stage.

Stage 2(b): Falling-rate period

The falling-rate period starts in the partially saturated stage, since $\tau_{CR} < \tau_U$. The pressure and moisture distributions at the start of stage 2(b) correspond to those at the end of stage 2(a). Note that a combination of the pressure distributions within the partially saturated stage in the ranges $\tau_E \le \tau \le \tau_{CR}$ and $\tau_{CR} \le \tau \le \tau_U$ is the same as the one shown in Fig. 3. During the falling-rate period, the moisture concentration at the surface of the plate remains at the equilibrium value so that eq. (15) can be solved numerically using conditions (16a), (16b) (for FRP), and (16c), to obtain the moisture distribution in the plate for the period from τ_{CR} to τ_U as shown in Fig. 6.

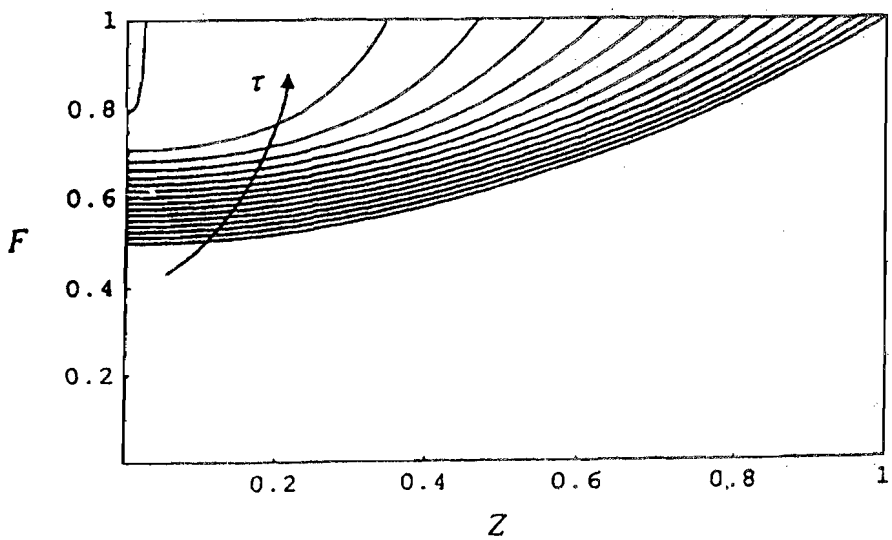

Fig. 3. Pressure distribution in the saturated zone of the partially saturated stage

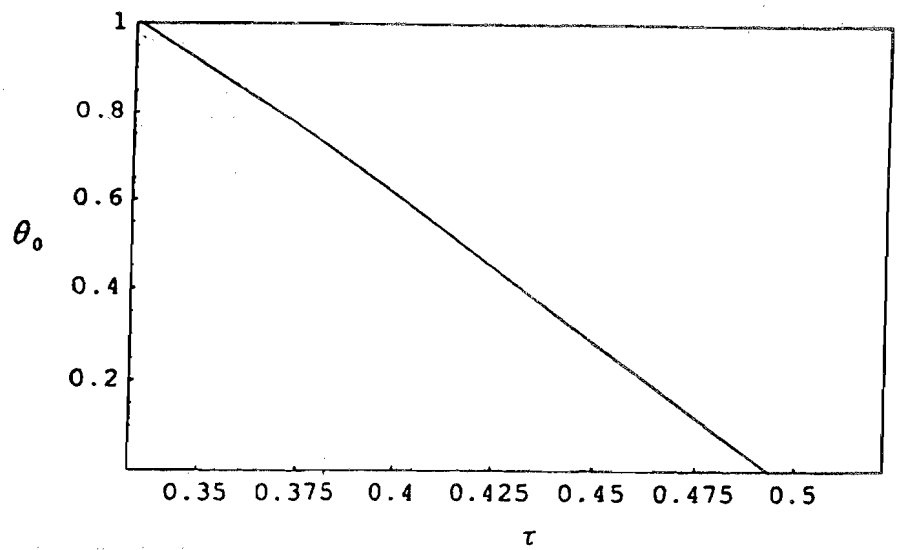

Fig. 4. Moisture concentration at the surface of the plate during the partially saturated stage (Case 1).

Stage 3: Fully unsaturated stage

When $Z_i(\tau)$ decreases to zero, the saturated zone of the partially saturated stage is obliterated and the fully unsaturated stage begins. The rescaled dimensionless transport equation in this stage may then be expressed as

$$\frac{\partial\theta}{\partial\tau}=\frac{\partial^2\theta}{\partial\xi^2} \qquad 0<\xi<1 \qquad (21)$$

with the corresponding conditions

$$\tau=\tau_U: \qquad \theta=\theta_U(\xi,\tau_U) \qquad (22a)$$

$$\xi=0: \quad \begin{cases} \text{CRP}: & \dfrac{\partial\theta}{\partial\xi}=\mu \\ \text{or} & \\ \text{FRP}: & \theta=0 \end{cases} \qquad (22b)$$

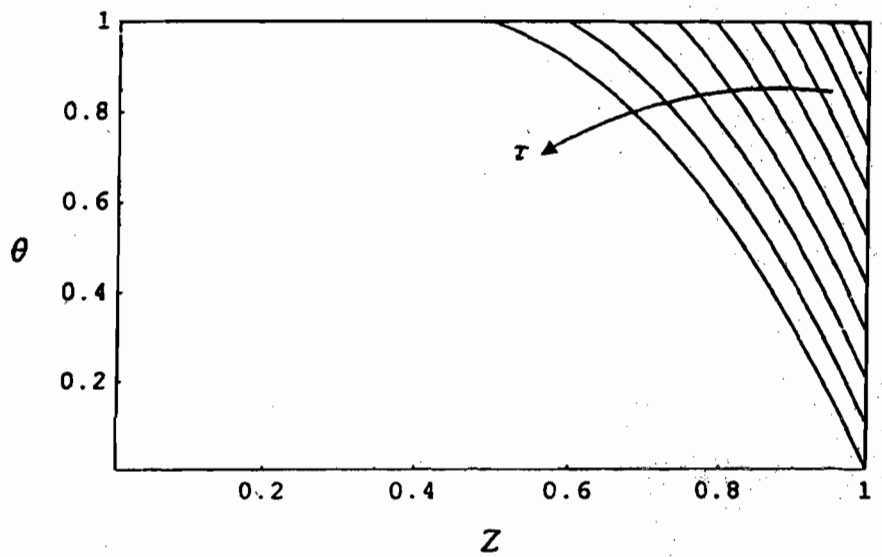

Fig. 5. Moisture distribution during the constant-rate period in the partially saturated stage (Case 1).

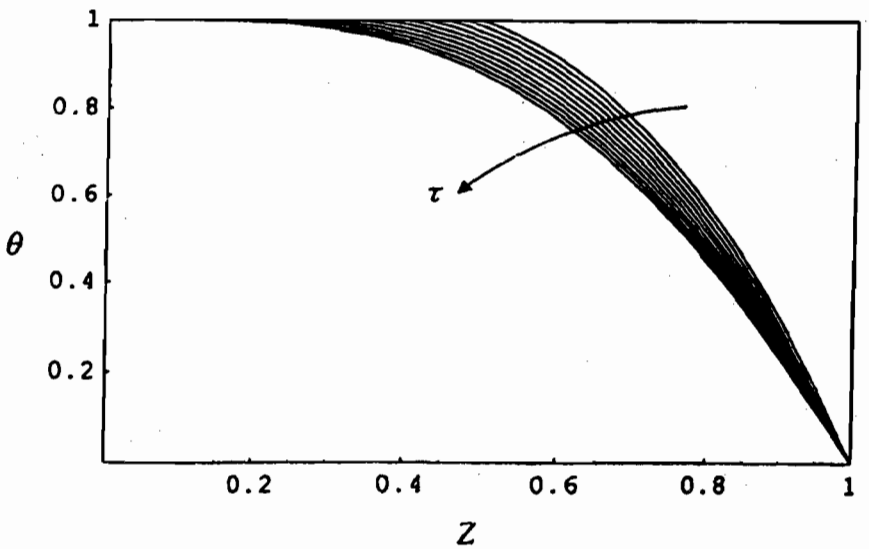

Fig. 6. Moisture distribution during the falling-rate period in the partially saturated stage (Case 1).

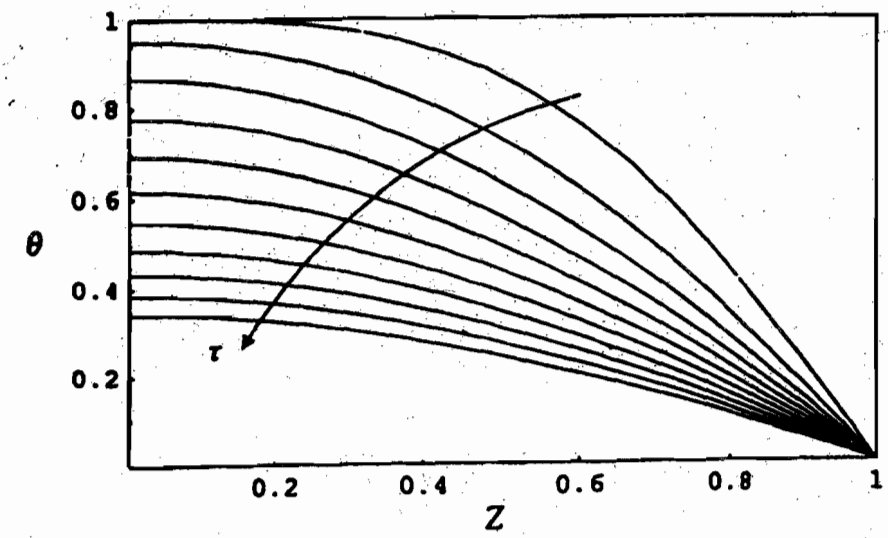

Fig. 7. Moisture distribution during the falling-rate period in the fully unsaturated stage (Case 1).

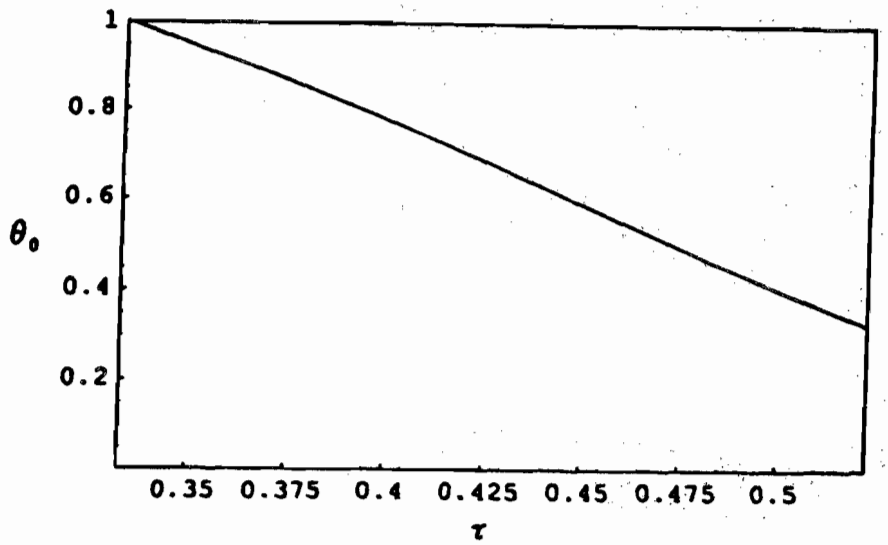

Fig. 8. Moisture concentration at the surface of the plate during the partially saturated stage (Case 2).

$$\xi = 1: \qquad \frac{\partial \theta}{\partial \xi} = 0 \tag{22c}$$

The moisture distribution at the beginning of the fully unsaturated stage corresponds to that at the end of stage 2(b), which (for $\beta = 2$, $\lambda = 1$, $\mu = 3.5$) has already entered the falling-rate period. Equation (21) can then be solved numerically using conditions (22a), (22b) (for FRP), and (22c), to obtain the moisture distribution in this stage as shown in Fig. 7. Thus the moisture distribution everywhere in the plate approaches the equilibrium value asymptotically at the end of drying.

Case 2. When the critical point occurs in the fully unsaturated stage

In this case, the drying intensity μ is taken to be 2, but the values of β and λ remain the same as in Case 1. Thus the pressure distribution in the saturated and partially saturated stages are the same as in Case 1, as is the evolution of the interface position and the dimensionless time for the end of the partially saturated stage.

Stage 2: Partially saturated stage

Stage 2(a): Constant-rate period

Since the constant-rate period continues from the saturated stage, through the partially saturated stage, into the fully unsaturated stage, eq. (15) can be solved numerically using conditions (16a), (16b) (for CRP), and (16c). The constant-rate period ends when the moisture concentration at the surface of the plate falls to the equilibrium value; that is $\theta = 0$ at $Z = 1$. Figure 8 shows a plot of θ_0 (the moisture concentration at the surface of the plate) against τ in the dimensionless time range $\tau_E \le \tau \le \tau_U$. It may be seen from Fig. 8 that θ_0 would fall to zero at a dimensionless time greater than τ_U, indicating that the constant-rate period extends into the fully unsaturated stage for this value of μ. Figure 9 shows the moisture distribution in the plate during the constant-rate period in the partially saturated stage for the period from τ_E to τ_U. Thus the moisture distribution is uneven, with higher moisture further from the drying face; the moisture concentration at the interior of the evaporative front remains at $\theta = 1$ (the fractional saturation of the pores) and the pressure remains at $F = 1$ as the evaporative front recedes through the material during the partially saturated stage.

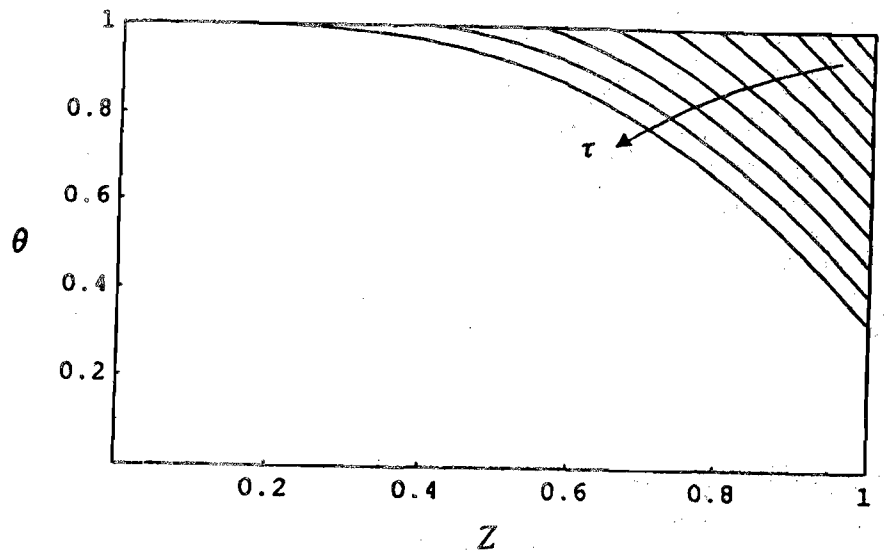

Fig. 9. Moisture distribution during the constant-rate period in the partially saturated stage (Case 2).

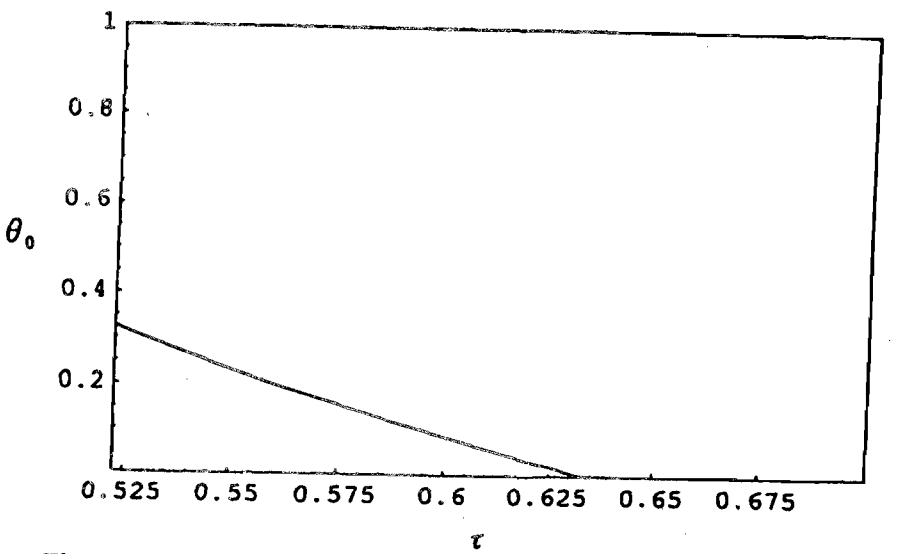

Fig. 10. Moisture concentration at the surface of the plate during the fully unsaturated stage (Case 2).

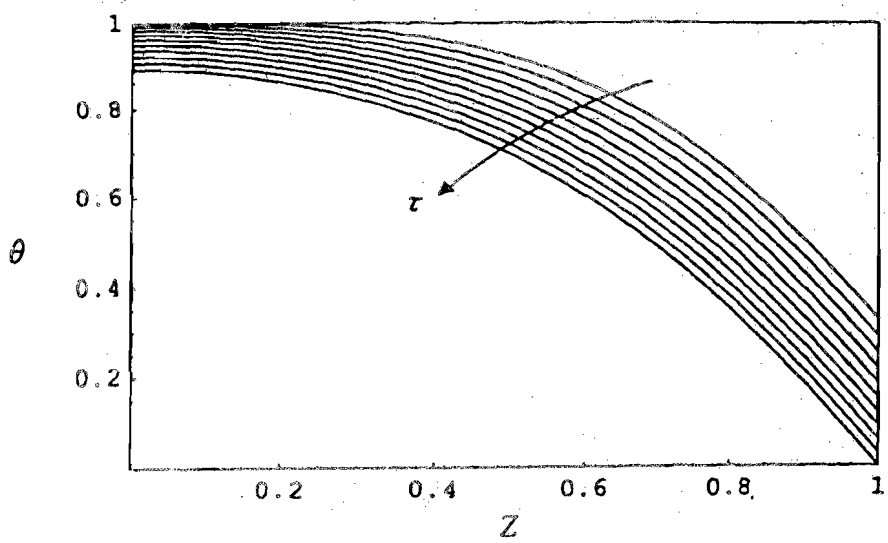

Fig. 11. Moisture distribution during the constant-rate period in the fully unsaturated stage (Case 2).

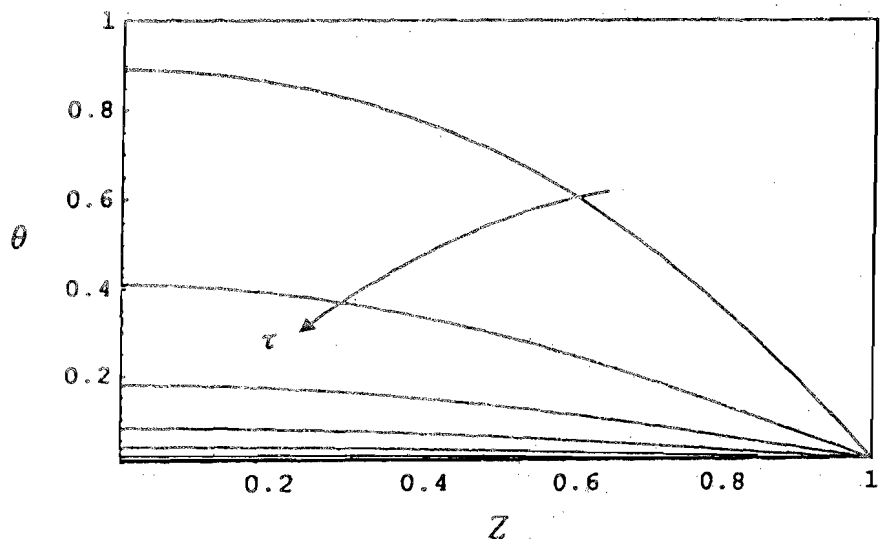

Fig. 12. Moisture distribution during the falling-rate period in the fully unsaturated stage (Case 2).

Stage 3 :Fully unsaturated stage

Stage 3(a): Constant rate period

The moisture distribution at the beginning of stage 3(a) corresponds to that at the end of stage 2(a). Since the rate of evaporation is still constant in the fully unsaturated stage, eq. (21) can be solved numerically using conditions (22a), (22b) (for CRP), and (22c). Figure 10 shows a plot of θ_0 against τ in a dimensionless time range from τ_U to $\tau = 0.7$, from which it may be seen that the constant-rate period ends at $\tau_{CR} \approx 0.633$ (obtained numerically), where τ_{CR} is the dimensionless critical time. Thereafter, the moisture concentration at the surface of the plate remains at the equilibrium value and the falling-rate period begins. Figure 11 shows the moisture distribution in the plate during the constant-rate period in the fully unsaturated stage from τ_U to τ_{CR}.

Stage 3(b): Falling-rate period

The moisture distribution at the beginning of stage 3(b) corresponds to that at the end of stage 3(a). Equation (21) can then be solved numerically using conditions (22a), (22b) (for FRP), and (22c), to obtain the moisture distribution during the falling-rate period in this stage of drying for the period from τ_{CR} to $\tau = 4$ as shown in Fig. 12. The moisture distribution everywhere in the plate approaches the equilibrium value asymptotically at the end of drying.

CONCLUSION

An analysis based on a three-stage drying process has been presented for the pressure and moisture distributions during drying of a flat plate with a fixed base. In this analysis, when the capillary tension in the liquid at the surface of a drying body reaches its maximum value, the liquid meniscus is drawn into the body and the material is only partially saturated. The constant-rate period continues until the moisture concentration at the surface of the body drops to the equilibrium value. Fluid transport through pores of the body is assumed to obey Darcy's Law in the saturated region, while moisture transport in the unsaturated region is modelled by a Fickian diffusion equation. Although models for the pressure and moisture distributions during drying of a flat plate exist in the literature (e.g. Scherer (1987a, 1987b, 1990); Sherwood (1931); Gilliland and Sherwood (1933); Puyate (1999, 2003a)), the present composite model offers a more complete description of a drying process, which takes into account the receding evaporative front.

The pressure distribution during the saturated stage is non-uniform, with higher pressure further from the drying face. During the partially saturated stage, the material is divided by the receding drying front into saturated and unsaturated zones; the pressure distribution in the saturated zone of the partially saturated stage is uneven, showing characteristics similar to those in the saturated stage, but the pressure at the evaporative front remains at the minimum value P_{min} as it recedes through the plate. The critical point occurs in the partially saturated stage in Case 1 (with $\beta = 2$, $\lambda = 1$, and $\mu = 3.5$), while the critical point occurs in the fully unsaturated stage in Case 2 (with $\beta = 2$, $\lambda = 1$, and $\mu = 2$). The moisture distributions during the constant-rate period in the partially saturated and fully unsaturated stages are uneven, with higher moisture further from the drying face. During the falling-rate period, the moisture concentration at the surface of the plate remains at the equilibrium value, while the moisture distribution everywhere in the plate approaches the equilibrium value at the end of drying.

ACKNOWLEDGEMENT

I would like to thank C. J. Lawrence for his contribution to this paper.

REFERENCES

Gilliland, E. R., and Sherwood, T. K., 1933. The drying of solids VI, Industrial and Engineering Chemistry, 25: 1134-1136.

Puyate, Y. T., 1999. Diffusion in Fine Tubes and Pores, Ph.D. Thesis, University of London.

Puyate, Y. T., 2003a. A receding evaporative front model for the drying characteristics of a flat plate I: Theory, submitted to Global Journal of Pure and Applied Sciences.

Puyate, Y. T., 2003b. A receding evaporative front model for the drying characteristics of a flat plate II: Stress and strain development, submitted to Global Journal of Pure and Applied Sciences.

Scheidegger, A. E., 1974. The Physics of Flow in Porous Media, 3rd ed., University of Toronto Press, Toronto, Cnada.

Scherer, G. W., 1987a. Drying gels II: Film and flat plate, Journal of Non-Crystalline Solids, 89: 217 - 238.

Scherer, G. W., 1987b. Drying gels V: Rigid gels, Journal of Non-Crystalline Solids, 92: 122 - 124.

Scherer, G. W., 1990, Theory of drying, Journal of the American Ceramic Society, 73: 3 - 14.

Sherwood, T. K., 1929. The drying of solids I, Industrial and Engineering Chemistry, 21: 12-14.

Sherwood, T. K., 1931. Application of theoretical diffusion equations to the drying of solids, *Trans. AIChE*, 27: 190 - 200.